We are IntechOpen,
the world's leading publisher of
Open Access books
Built by scientists, for scientists

4,800
Open access books available

122,000
International authors and editors

135M
Downloads

Our authors are among the

154
Countries delivered to

TOP 1%
most cited scientists

12.2%
Contributors from top 500 universities

CLARIVATE ANALYTICS
BOOK CITATION INDEX
INDEXED

WEB OF SCIENCE™

Selection of our books indexed in the Book Citation Index
in Web of Science™ Core Collection (BKCI)

Interested in publishing with us?
Contact book.department@intechopen.com

Numbers displayed above are based on latest data collected.
For more information visit www.intechopen.com

Mechanisms of αIIbβ3 Biogenesis in the Megakaryocyte: A Proteomics Approach

Amanda Chen[1], Haiqiang Yu[2], Haiteng Deng[2] and W. Beau Mitchell[1]
[1]Laboratory of Platelet Biology, New York Blood Center
[2]Proteomics Resources Center, The Rockefeller University
USA

1. Introduction

Platelets play a central role in hemostasis and thrombosis, initiating clot formation in response to vessel wall damage. Platelet aggregates are formed at sites of injury by the binding and crosslinking of the integrin αIIbβ3 to fibrinogen, von Willebrand factor and other soluble ligands. Platelets also form pathological thrombi, and the resulting arterial occlusion can lead to myocardial infarction or stroke. Inhibition of αIIbβ3 binding can decrease the formation of pathologic thrombi, and αIIbβ3 has become an important pharmacological target. Anti-αIIbβ3 therapies have been highly successful in preventing death following myocardial infarction and percutaneous arterial stent placement.(Topol, Lincoff et al. 2002; De Luca, Ucci et al. 2009) However, attempts to design novel, orally available anti-αIIbβ3 agents have been hampered by what appears to be paradoxical activation of αIIbβ3 by the drug, in some cases leading to an increased risk of mortality in patients who received the drug.(Quinn, Plow et al. 2002)

A novel approach to manipulating αIIbβ3 would be to perturb its post-translational processing and trafficking within the megakaryocyte, prior to platelet formation. Like most membrane proteins, αIIbβ3 is formed by concerted processes of protein sorting and trafficking. Some of the mechanisms underlying αIIbβ3 biogenesis and expression in megakaryocytes have been described, such as the calnexin cycle of protein quality control.(King and Reed 2002; Tiwari, Italiano et al. 2003; El.Golli, Issertial et al. 2005; Lo, Li et al. 2005) Clues to the stringent protein quality control of αIIbβ3 biogenesis come from the study of patients with defective or absent αIIbβ3, who manifest the mucocutaneous bleeding disorder Glanzmann thrombasthenia. A subset of patients with mutations in the αIIb gene produce full-length αIIb that retains the ability to form a complex with β3 but is retained within the cell and degraded, resulting in disease. These patients demonstrate the existence of stringent quality control mechanisms acting post-translationally to control αIIbβ3 biogenesis and expression. A clearer understanding of these mechanisms may lead to new possibilities of anti-integrin therapy.

Toward the goal of identifying proteins involved in αIIbβ3 biogenesis we performed a proteomic analysis of proteins interacting with αIIb in megakaryocytes cultured from human umbilical cord blood (UCB) and in HEK293 cells expressing αIIb and β3.

Megakaryocyte proteins were captured by poly-histidine tagged αIIb, or by photoreactive crosslinking followed by immunoprecipitation with anti-αIIb mAbs, and analyzed by mass spectrometry.

The αIIb and b3 subunits are synthesized as a single-chain precursors in the chaperone-rich folding environment of the endoplasmic reticulum (ER) (Fig 1). The precursor αIIb, pro-αIIb, is glycosylated under control of the calnexin cycle of protein folding. The β3 precursor is also glycosylated but does not appear to interact with the calnexin cycle. The two precursors heterodimerize to briefly form pro-αIIbβ3, and then pro-αIIb is cleaved by one or more members of the furin family of proteases in the Golgi. Cleavage of pro-αIIb to mature αIIb marks the exit of αIIb from the ER, and this cleavage occurs only when pro-αIIb is in complex with β3.(Bray, Rosa et al. 1986; Rosa and McEver 1989) Both αIIb and β3 are synthesized in excess of what will finally be processed to mature αIIbβ3. The calnexin cycle exerts stringent quality control over αIIb production and up to one half of all pro-αIIb is targeted to the proteasome for degradation in megakaryocytes. Excess β3 is degraded by a non-proteasomal mechanism. Inhibition of the proteasome in megakaryocytes resulted in a build-up of pro-αIIb that was not being degraded, but had no apparent effect on the level of mature αIIb in the αIIbβ3 complex. Thus, the expression level of mature αIIbβ3 is not simply a result of the stoichiometry of production vs. degradation. Rather there appears to be a concerted mechanism that controls how much pro-αIIbβ3 will be converted into mature αIIbβ3, and this mechanism is not grossly responsive to excessive levels of pro-αIIb or β3.
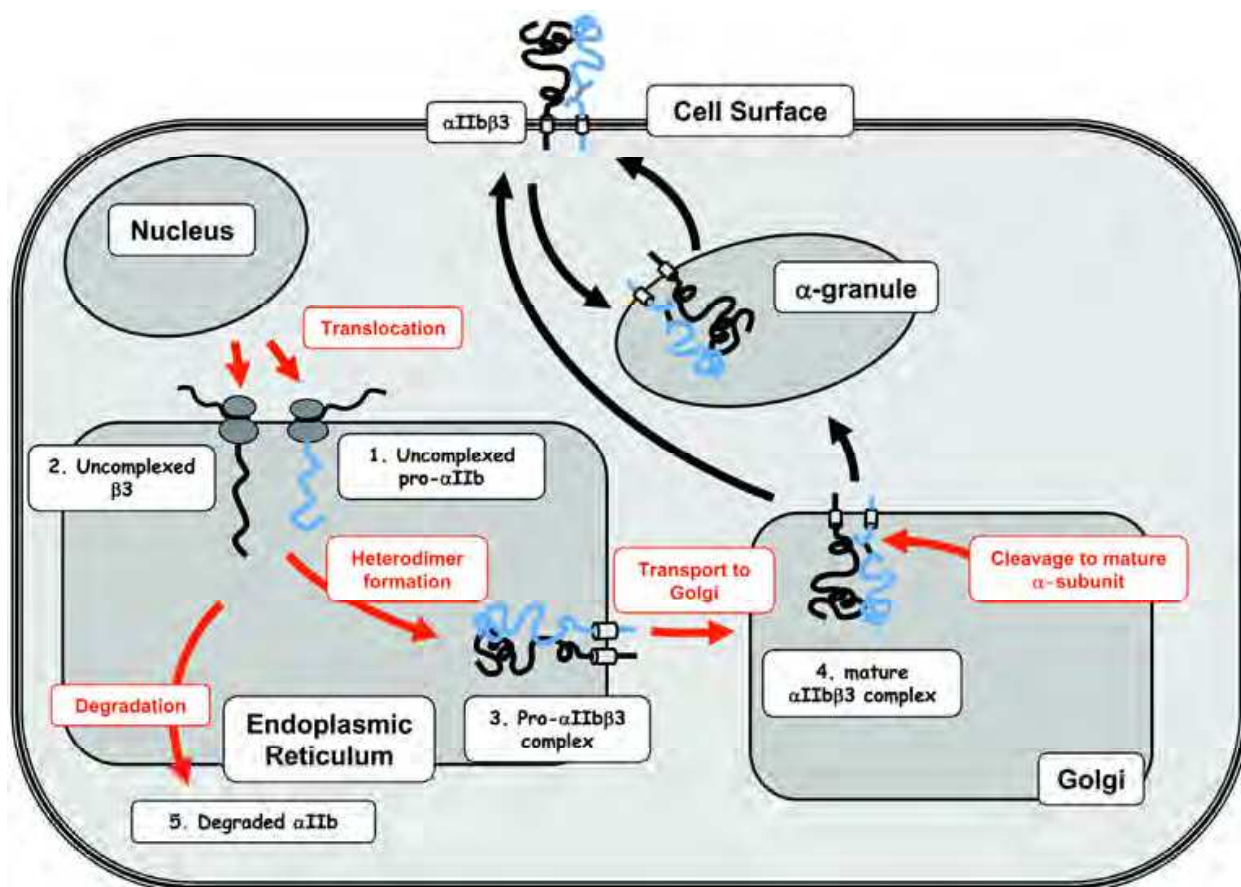

Fig. 1. Biogenesis of αIIbβ3

We hypothesized that whatever proteins underlie this mechanism must be interacting with pro-αIIb and/or pro-αIIbβ3 complex, but not with the mature αIIbβ3 complex. We chose a proteomics approach to identify these interacting proteins. In order to enrich our assay for proteins that preferentially bound pro-αIIb or pro-αIIbβ3, we used an αIIb subunit harboring R858G and R859G mutations that eliminates furin cleavage and traps αIIb in its pro-αIIb form.(Kolodziej, Vilaire et al. 1991) This αIIbR858G/R859G construct can form a complex with β3, but only in small amounts compared to normal αIIbβ3. In addition, while some of the mutant αIIbβ3 complexes reach the cell surface and can mediate adherence to immobilized fibrinogen, the proportion of αIIbR858G/R859G reaching the surface is very small compared to normal αIIb.(Kolodziej, Vilaire et al. 1991) Thus, αIIbR858G/R859G is a "nearly normal" mutant αIIb subunit that is primarily retained within the cell, making it a useful bait to capture the proteins involved in that process.

The hsp40 type chaperone protein, DNAJC10, was captured by both the normal αIIb and αIIbR858G/R859G subunits, and was evaluated as a putative αIIb interacting protein.. We report that DNAJC10 interacted with pro-αIIb and β3 in megakaryocytes, and appears to promote the degradation of pro-αIIb. Notably, while αIIbβ3-DNAJC10 interaction was evident in megakaryocytes, specific interaction was not detectable in HEK293 cells transfected with αIIb cDNA, suggesting megakaryocyte specificity. Knockdown of DNAJC10 by siRNA increased αIIbβ3 surface expression in UCB derived megakaryocytes, indicating that DNAJC10 negatively regulates αIIbβ3 surface expression. Thus, DNAJC10-αIIb interaction represents a novel post-translational mechanism regulating αIIbβ3 surface expression.

2. Materials and methods

2.1 Antibodies

The antibodies used in this study were: 10E5 (anti-αIIbβ3 complex); B1B5 (anti-αIIb);7H2 and B36 (anti-β3) (all 4 generous gifts from Dr Barry Coller); CA3 (anti-αIIb), anti-V5 epitope, and anti-Myc epitope (all three Millipore, Temecula,CA); anti-DNAJC10 (Genetex, Irvine, CA); M148 (anti-αIIb) (Santa Cruz Biotechnology, Santa Cruz, CA); mouse IgG, and rabbit IgG (both Jackson ImmunoResearch Inc, West Grove, PA).

2.2 Human Umbilical Cord Blood culture

This study used human UCB from the US National Cord Blood Bank that was deemed not suitable for clinical use due to low white blood cell number. Mothers who donate their UCB to the National Cord Blood Bank sign a consent giving permission to donate the UCB to research if it is inadequate for clinical use and will be discarded. Because the donated units are completely de-identified and are not collected prospectively specifically for research, the New York Blood Center Institutional Review Board (IRB), which oversees research ethics at the National Cord Blood Bank, considers their use exempt from IRB review. Human UCB was prepared as previously described.(Mitchell, Li et al. 2006) Briefly, leukocytes were separated from 1-3 units of human UCB judged to be inadequate for clinical purposes (generously provided by the New York Blood Center) by Dextran 70 sedimentation (Amersham Biosciences, Piscataway, NJ) for 1h, and then enriched for CD34+ progenitor

cells by negative selection using a combination of antibodies against maturation/lineage-specific markers (RosetteSep, StemCell Technologies, Vancouver, BC) concomitant with density sedimentation using Ficoll-Paque Plus (Amersham Biosciences, Piscataway, NJ). These cells were cultured in serum-free medium (StemCell Technologies, Vancouver, BC) with 50 ng/ml thrombopoietin (TPO) plus 1 ng/ml SCF (both Millipore, Temecula,CA) for 3 days in 10 cm dishes in a 37°C incubator. At this point a portion of the cells will have died. The remaining living population of larger cells was gently washed and replated in fresh media with the same cytokines in 10 cm dishes and left until use (Day 8 or 9). Fresh media was added on day 6. We have previously reported that under these conditions the UCB differentiate into a population of large cells with > 90% expressing αIIbβ3, > 80% expressing GPIb, about 50% expressing α2β1.(Mitchell, Li et al. 2007) For experimental use the cells were gently harvested, pelleted at 300 rpm for 5 min, or let settle by gravity, and gently resuspended in the appropriate buffer.

2.3 HEK293 cell culture

HEK293 cell lines (American Type Culture Collection (ATCC), Manassas, VA) that stably expressed human αIIbβ3 receptors were established as previously described.(Mitchell, Li et al. 2006) Transfections were performed using Lipofectamine 2000 (Gibco-BRL, Carlsbad, CA) according to the manufacturer's instructions, followed by selection in media containing 500 μg/ml G418 for 2-4 weeks. To obtain a population of cells uniformly expressing high levels of αIIbβ3, cells were labeled with the mAb 10E5 (anti-αIIbβ3) and sorted using a MoFlo cell sorter (Beckman Coulter, Fullerton, CA).

2.4 Immunoprecipitation and biosynthetic labeling

Samples were prepared as previously described and all steps were performed on ice unless otherwise stated.(Mitchell, Li et al. 2006) Briefly, cells (either day 8 megakaryocytes derived from UCB cells or HEK293 cells) were lysed in 1% Brij 98 lysis buffer containing protease inhibitors and 20uM N-methylmaleimide (NEM). Lysates were precleared with protein-G Sepharose beads (Amersham Biosciences, Piscataway, NJ), and then equivalent amounts of protein, usually 400 μg, were incubated one h at 4°C with one or more of the antibodies listed above (4 μg/reaction). Samples were incubated with protein-G Sepharose beads for one h at 4°C, washed twice, and incubated with SDS sample buffer for 10 min at 100°C. Reduced samples contained 10% beta mercaptoethanol (Sigma, Thermo Scientific, Rockford, IL). Samples were subjected to SDS-PAGE on 7% gels, and the gels were either stained for mass spectrometry identification (described below) or transferred to PVDF membranes for immunoblotting. Non-specific binding was determined by performing parallel immunoprecipitation with mouse or rabbit IgG in each experiment. In preliminary experiments, the production of αIIbR858G/R859G and β3 was confirmed in the transfected HEK293 cell line by immunoprecipitation with both anti-αIIb and anti-β3 mAbs followed by immunoblot. For biosynthetic labeling, cells were incubated for 30 min at 37°C in methionine/cysteine-free medium, followed by pulse-labeling for 15 min at 37ºC in medium containing ^{35}S-methionine/cysteine (300 μCi/10 cm plate). The pulse was terminated by incubation in medium containing unlabeled methionine/cysteine (1 mg/ml each) and the cells were incubated at 37 °C until lysis in 1% Triton-X 100 lysis buffer. Following cell lysis, supernatants were prepared as above. Gels were dried and exposed to film. For inhibition of

the proteasome cells were incubated in the proteasome inhibitor MG132 (10 μM)(Sigma_Aldrich, St Louis, MO) in normal growth medium at 37C and then immediately lysed.

2.5 Histidine-tag/Nickel bead pulldown assay

HEK293 cells expressing poly-histidine tagged αIIb cDNA (in vector pEF1/V5-His) and β3 cDNA (in vector pcDNA3.1)(Mitchell, Li et al. 2007) were lysed in 1% Triton, 150 mM NaCl, 10 mM imidazole buffer (lysis buffer) on ice for 30 m, centrifuged for 30m at 4C, and then the supernatant was reacted with 50 μl of a 6:4 slurry of Ni beads:imidazole buffer (Qiagen, Inc. Valencia, CA) to bind the histidine-tagged subunits to the nickel beads. After incubating for 30 m the beads were washed four times with 10 mM imidazole lysis buffer by using a magnetic chamber to isolate the beads. Next, fresh whole cell lysates (1 mL) of UCB-derived megakaryocytes in 1% Triton, 150 mM NaCl, 10 mM imidazole buffer were incubated with the washed, Ni-bound αIIb for 1 h, and then the beads were washed twice with 1 mL lysis buffer containing 20 mM imidazole. Ni-bound proteins were eluted with 250 mM imidazole and the entire eluate was subjected to SDS-PAGE on a 7% gel followed by staining with Imperial Stain (Pierce, Thermo Scientific, Rockford, IL). Control experiments were run in parallel in which no megakaryocyte lysate was added to the beads, but all other steps remained the same. These controls aimed to identify the remaining HEK293 cell proteins still bound to either the beads or to αIIb after the washing steps, before incubation with megakaryocyte lysate. Experimental and control gels were run simultaneously, and the lanes were excised and analyzed by mass spectrometry.

2.6 Photocrosslinking amino acids

UCB cells were cultured as described above for eight days, then were washed and incubated for 24 hours in leucine- and methionine- free medium containing photoreactive methionine and leucine, dialyzed FBS (both Pierce, Thermo Scientific, Rockford, IL), and 50 ng/ml TPO (Millipore, Temecula,CA). The cells were exposed to 345 nm UV light for 15 minutes to crosslink the photoreactive amino acids, and harvested immediately, according to manufacturer's instructions. Whole cell lysates were immunoprecipitated with antibodies specific for αIIb or β3, and the proteins were separated by SDS-PAGE using the same protocol as for the histidine-tag affinity capture. Controls were simultaneously immunoprecipitated with non-immune IgG. Experimental and control lanes were excised and analyzed by mass spectrometry.

2.7 RNAi

HEK293 cells stably expressing high levels of αIIb and β3 were transfected with 100 nM siRNA duplexes (Dharmacon, Thermo Scientific, Rockford, IL and Qiagen, Valencia, CA) using Dharmafect-1 reagent (Dharmacon, Thermo Scientific, Rockford, IL), then analyzed by flow cytometry using a FacsCanto (Becton Dickenson,) at 48-96 h after transfection. Cultured UCB cells were transfected twice, on culture days 3 and 5, with 100 nM of siRNA duplexes or controls also using Dharmafect-1 reagent, and then analyzed 48 – 72 h later by flow cytometry. In order to identify individual transfected cells by FACS, cells were co-transfected with 10 nM of fluorescent-labeled non-coding siRNA (Qiagen, Valencia, CA). In

some experiments, Cy3-labeled siRNA duplexes were used (Dharmacon, Thermo Scientific, Rockford, IL). Controls were: no treatment, transfection reagent but no siRNA duplex, Cy3-labeled negative control siRNA duplex only (Qiagen), siControl non targeting siRNA duplex, and siRNA duplex against cyclophillin B (positive control) (both Dharmacon).

2.8 Quantitative RT-PCR

For analysis of RNA content, cells were collected in RNAlater (Applied Biosystems, Foster City, CA) and RNA was purified using the RNEasy mini kit (Qiagen, Valencia, CA). For some analyses, siRNA transfected cells were sorted for expression of the fluorescent marker using a MoFlo sorter, and the sorted cells were subjected to QRT-PCR. Analysis was performed on an ABI 7900 or an ABI 7700 thermocycler/ fluorescence analyzer (Applied Biosystems, Foster City, CA) using the SYBR green probe (Qiagen or Invitrogen) and Quantitect primer assays (Qiagen). Relative mRNA levels were calculated using the ΔΔCt method that corrects for GAPDH expression in all samples. Fold-reduction was corrected for percent transfection in each experiment.

2.9 Immunofluorescence analysis

Mks were cytospun onto poly L-lysine-coated glass coverslips and fixed in methanol for 5 minutes at RT. Cells were then washed with saponin buffer (PBS containing 0.02% BSA, 0.005% saponin), then blocked with saponin buffer for 1 hour at RT. Cells were then incubated with the primary antibody diluted in saponin buffer for 1 hour at RT. After washing with PBS, cells were incubated with the appropriate conjugated secondary antibody in PBS for 1 hour at RT. Specimens were mounted with Prolong gold (Invitrogen). Images were acquired using a Zeiss LSM 510 META (Axiovert 200M Inverted Microscope Stand) confocal laser scanning microsope through a 100x objective. Each set of staining conditions was repeated 3 times. Background fluorescence was measured by incubating fixed cells with the secondary antibody only and then acquiring images with the exact settings used to obtain the experimental images.

2.10 Mass spectrometry data analysis

The protein gel bands were excised from the SDS-PAGE. The gel bands were reduced with 10 mM of DTT and alkylated with 55 mM iodoacetamide, and then digested with Sequence Grade Modified Trypsin (Promega, Madison, Wisconsin) in ammonium bicarbonate buffer at 37° overnight.(Kumarathasan, Mohottalage et al. 2005) The digestion products were extracted twice with 0.1% trifluoroacetic acid and 50% Acetonitrile and 1.0% trifluoroacetic acid respectively. The extracted mixture was dried by Speed-Vac and redisolved in 10 μL 0.1% trifluoroacetic acid. Half of the extracts were injected by LC-MS/MS analysis. For LC-MS/MS analysis, each digestion product was separated by a 60 min gradient elution with the Dionex U3000 capillary/nano-HPLC system (Dionex, Sunnyvale, California) at a flow rate of 0.250 μL/min that is directly interfaced with the Thermo-Fisher LTQ-Obritrap mass spectrometer (Thermo Fisher, San Jose, California) operated in data-dependent scan mode. The analytical column was a home-made fused silica capillary column (75 μm ID, 100 mm length; Upchurch, Oak Harbor, Washington) packed with C-18 resin (300 A, 5 μm, Varian, Palo Alto, California). Mobile phase A consisted of 0.1% formic acid, and mobile phase B

consisted of 100% acetonitrile and 0.1% formic acid. The 60 min gradients with 250 nL/min flow rate for B solvent went from 0 to 55% in 34 minutes and then in 4 min to 80%. The B solvent stayed at 80% for another 8 min and then decreased to 5% in 8 min. Another 6 min was used for equilibration, loading and washing. The mass acquisition method was one FT-MS scan followed by 6 subsequent MS/MS scan in the ion trap. The FT-MS scan was acquired at resolution 30,000 in the Orbi-trap. The six most intense peaks from the FT full scan were selected in the ion trap for MS/MS. The selected ions were excluded for further selection for 180 seconds. The following search parameters were used in all MASCOT searches: maximum of 1 missed trypsin cleavages, cysteine carbamidomethylation, methionine oxidation. The maximum error tolerance for MS scans was 10 ppm for MS and 1.0 Da for MS/MS respectively. Proteins were designated as "hits" if they matched at least 2 distinctive peptides with a MASCOT score of at least 40. For proteins matching the same sets of peptides, only the protein with the greater percentage of coverage was selected. In the one case where 2 isoforms could not be distinguished (HSP70A/B), both proteins are reported. Proteins identified in the control gels were considered "negative," and these proteins were removed from further analysis. The interaction data were further analyzed using the Cytoscape(Cline, Smoot et al. 2007) software and publically available protein interaction databases (e.g. INTACT, NCBI, UniProt) to generate a network of first-degree interactions with αIIb. The network was further expanded to include proteins that were previously reported to interact with αIIb and known interactions between any of the proteins identified in our primary assays.

2.11 Statistical analysis

Flow cytometry data was summarized as the geographic mean fluorescence intensity (MFI) of antibody binding, and normalized to the MFI of control siRNA treated cells, so that the experimental MFI is expressed as a percentage of the control MFI. The overall percent change of the replicates was expressed as the average percent change +/- the confidence interval. The two-sided, paired t-test was used to determine whether there were differences in antibody binding between the different experimental groups. In the siRNA experiments, relative mRNA levels were calculated using the ΔΔCt method that corrects for GAPDH expression.

3. Results

3.1 The αIIb interactome

Proteins putatively interacting with αIIb were isolated from UCB derived megakaryocytes and from HEK293 cells expressing αIIbβ3, and these proteins were analyzed by mass spectrometry. Samples were processed by the two methods depicted in **Figure 2**. In the first method, recombinant αIIb or αIIbR858G/R859G subunits bearing a polyhistidine tag were expressed in HEK293 cells along with normal β3. The cells were lysed with 1% Triton buffer, and the lysates were reacted with Ni beads that bind polyhistidine. The Ni beads were washed using a magnetic separator to reduce non-specific binding to the Ni-bound αIIb, and then incubated with fresh whole cell lysate of umbilical cord blood derived megakaryocyte. Since we are interested in the early process of αIIbβ3 formation and intracellular trafficking we used megakaryocytes at day 8 or 9 of culture; at that point in our

system αIIbβ3 is highly expressed but there is not yet any proplatelet formation. The Ni-bound histidine-tagged αIIb and αIIb-bound proteins were washed twice and then were eluted from the Ni beads with 250 mM imidazole in a 1% Triton buffer. Simultaneous control experiments were performed without megakaryocyte lysate in order to identify proteins non-specifically binding to either the Ni beads or the polyhistidine tag. The proteins thus collected were separated by one dimensional SDS-PAGE on a 7% gel. After staining, the experimental and control lanes were cut out and analyzed by mass spectrometry. This entire process was repeated in three separate experiments with normal αIIb, and in four separate experiments with αIIbR858G/R859G.
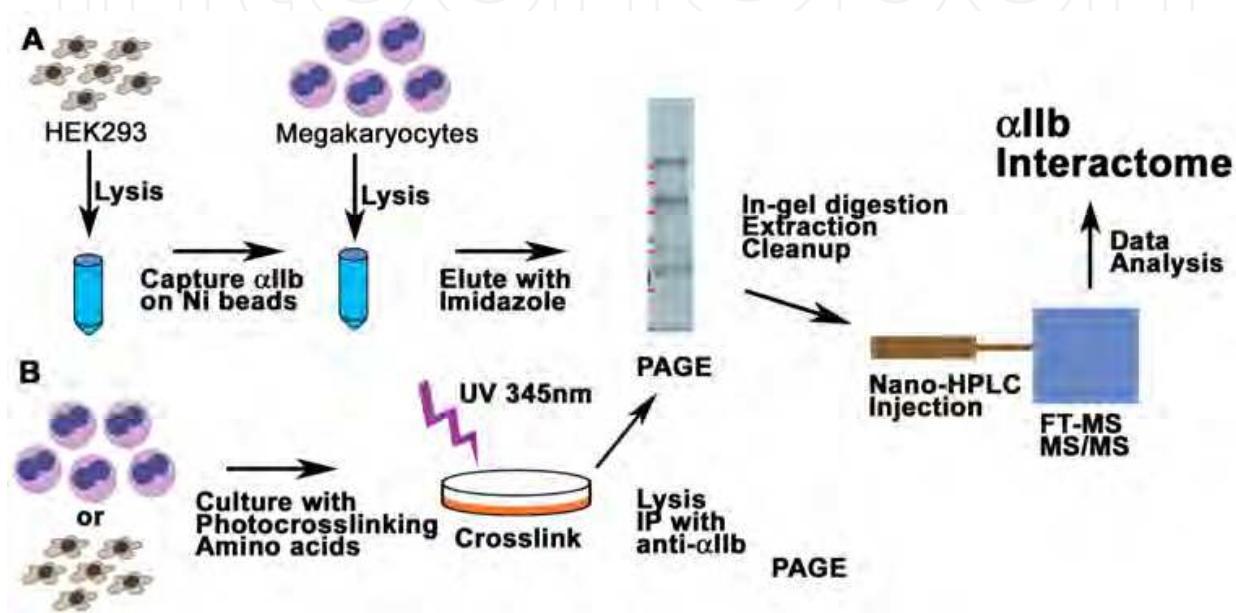

Fig. 2. Methods used to isolate and identify αIIb-interacting proteins. A): Polyhistidine-tagged αIIb subunits were captured on Ni beads and then incubated with whole cell lysate of day 8 UCB-derived megakaryocytes. Protein complexes thus captured were processed as described in the text, and then the proteins were identified by FT-MS and MS/MS. B) Crosslinking experiments were performed on day 8 UCB-derived megakaryocytes and transfected HEK293 cells. Cells were fed photoactivatable methionine and leucine, exposed to UV light and lysed immediately. Samples were processed for mass spectrometry as described.

The second strategy used photo-activated amino acids to crosslink αIIb to its binding partners (**Figure 2B**). UCB-derived megakaryocytes were starved for methionine and leucine, then fed photo-activatable methionine and leucine overnight, and then exposed to UV light to crosslink the amino acids of neighboring proteins. The megakaryocytes were immediately lysed and the αIIb-bound proteins were immunoprecipitated by anti-αIIb mAb. These proteins were separated by one dimensional SDS-PAGE and then the appropriate bands were cut out and analyzed by mass spectrometry. Because we were looking only for proteins crosslinked to αIIb, only the portions of the bands with $M_r > 120$ (M_r of the mature αIIb subunit) were analyzed. Five separate crosslinking experiments were performed with UCB-derived megakaryocytes and two on HEK293 cells expressing αIIbR858G/R859G and normal β3.

Minimum criteria for protein inclusion in data analysis were at least 2 distinctive peptides with a MASCOT score of at least 40, and absence of the protein in the control lanes. Importantly, since we were interested in proteins that are more abundant in the megakaryocyte than in HEK293 cells, even proteins known to interact with αIIbβ3, such as talin, were removed from the final results because they were present in the control lanes. Proteins identified in the Ni bead extraction experiments that are known to harbor natural polyhistidine sequences (such as the DEAH boxes) that could independently bind to the Ni beads were also excluded. Combining the results of both methods, 98 proteins were identified as potentially interacting with the normal αIIb subunit, and 79 proteins were identified as putatively interacting with the αIIbR858G/R859G subunit (Table 1). These 163 proteins putatively constitute a portion of the αIIb interactome, a network of protein-protein interactions relevant to the trafficking and function of αIIb in megakaryocytes (**Figure 3**).

Proteins Captured with αIIbR858G/R859G

Gene Symbol	Entrez Gene ID	SwissProt Acc No.	Protein Acc No.	Description	# Pep	% Cov	#. Expt
MYH9	4627	P35579 Q60FE2	gi|12667788	MYOSIN, HEAVY POLYPEPTIDE 9, NON-MUSCLE	70	45	4
LMNA	4000	P02545	gi|5031875	LAMIN A/C	37	61	3
HNRNPL*	3191	P14866 A6NIT8 Q6NTA2	gi|11527777	HETEROGENEOUS NUCLEAR RIBONUCLEOPROTEIN L	33	53	4
STIM1	6786	Q13586	gi|21070997	STROMAL INTERACTION MOLECULE 1	28	46	2
CKAP4	10970	Q07065	gi|19920317	CYTOSKELETON-ASSOCIATED PROTEIN 4	27	55	2
HSP90AB1	3326	P08238	gi|154146191	HEAT SHOCK PROTEIN 90kDa ALPHA, CLASS A MEMBER 1	21	36	1
SF3A1	10291	Q15459 B3KTT5	gi|53831995	SPLICING FACTOR 3A, SUBUNIT 1, 120kDa	16	32	1
HSPA1A*	3303	P08107 A8K5I0 Q8WWM7	gi|5123454	HEAT SHOCK 70kDa PROTEIN 1A	15	34	3
ATXN2L*	11273	A8K1R6 Q6PK16	gi|119572372	ATAXIN 2-LIKE	14	20	2
MYH10	4628	P35580 Q9BWG0	gi|41406064	MYOSIN, HEAVY POLYPEPTIDE 10, NON-MUSCLE	13	9	1
DNAJC10*	54431	Q8IXB1	gi|24308127	DNAJ (HSP40) HOMOLOG, SUBFAMILY C, MEMBER 10	13	21	3
PSPC1	55269	Q8WXF1	gi|109240550	PARASPECKLE COMPONENT 1	13	35	3
SFPQ	6421	P23246 Q86VG2	gi|119627829	SPLICING FACTOR PROLINE/GLUTAMINE-RICH (POLYPYRIMIDINE TRACT BINDING PROTEIN ASSOCIATED)	12	35	1
SF1*	7536	Q14820	gi|42544123	SPLICING FACTOR 1	12	20	2

Gene	ID	UniProt	gi	Description			
		Q15637					
HSPA5*	3309	P11021	gi|119608027	HEAT SHOCK 70kDa PROTEIN 5 (GLUCOSE-REGULATED PROTEIN, 78kDa)	11	37	4
HLF2	4057	P02788	gi|16198357	LACTOTRANSFERRIN	11	30	1
MYH11	4629	P35749 Q3MNF1 Q3MIV8 Q3MNF0	gi|119574312	MYOSIN, HEAVY POLYPEPTIDE 11	11	9	1
LTBP1	4052	Q14766 B7ZLY3	gi|46249414	LATENT TRANSFORMING GROWTH FACTOR BETA BINDING PROTEIN 1	10	8	2
PKM2*	5315	P14618	gi|127795697	PYRUVATE KINASE, MUSCLE	10	28	1
RAVER1*	125950	Q8IY67	gi|123173757	RAVER1	10	29	2
XIRP2	129446	A4UGR9 Q8NE71 Q2L6I2	gi|61696134	CARDIOMYOPATHY ASSOCIATED 3	10	16	1
ABCF1	23	A2BF75	gi|21759807	ATP-BINDING CASSETTE, SUB-FAMILY F (GCN20), MEMBER 1	9	14	1
POTEF	728378	A5A3E0	gi|153791352	POTE ANKYRIN DOMAIN FAMILY, F	9	8	1
HSP90AA1	3320	P07900 Q86SX1	gi|153792590	HEAT SHOCK PROTEIN 90kDa ALPHA, CLASS A MEMBER 1	8	13	3
ITGA2B*	3674	P08514	gi|119571981	INTEGRIN, ALPHA 2B (PLATELET GLYCOPROTEIN IIB OF IIB/IIIA COMPLEX, ANTIGEN CD41)	8	17	2
TF*	7018	Q06AH7 P02787	gi|110590597	TRANSFERRIN	8	18	2
SAP 62	8175	A0PJA6	gi|21361376	SPLICING FACTOR 3A, SUBUNIT 2, 66kDa	8	19	1
LYZ	4069	Q05DF2 Q15428	gi|4930023	LYSOZYME (RENAL AMYLOIDOSIS)	7	70	1
SMAD4	4089	P61626 B2R4C5 Q13485	gi|4885457	SMAD, MOTHERS AGAINST DPP HOMOLOG 4 (DROSOPHILA)	7	12	2
HSP90B1	7184	P14625	gi|4507677	HEAT SHOCK PROTEIN 90kDa BETA (GRP94), MEMBER 1	7	12	2
CANX	821	P27824	gi|10716563	CALNEXIN	6	13	1
LRP2	4036	Q7Z5C1 P98164 Q7Z5C0	gi|32816595	LOW DENSITY LIPOPROTEIN-RELATED PROTEIN 2	6	1	1
CCT3	7203	A6NE14 P49368 B3KX11	gi|14124984	CHAPERONIN CONTAINING TCP1, SUBUNIT 3 (GAMMA)	6	21	2
HSPA1L	3305	P34931	gi|21759781	HEAT SHOCK 70kDa PROTEIN 1-LIKE	5	15	2
NCL	4691	P19338	gi|189306	NUCLEOLIN	5	6	1

		B3KM80					
PIP	5304	P12273	gi|4505821	PROLACTIN-INDUCED PROTEIN	5	31	1
SLPI	6590	P03973	gi|4507065	SECRETORY LEUKOCYTE PEPTIDASE INHIBITOR	5	28	1
TPM1	7168	P09493 Q9Y427 O15513	gi|854189	TROPOMYOSIN 1 (ALPHA)	5	10	1
HECTD1	25831	Q9ULT8	gi|118498337	HECT DOMAIN CONTAINING 1	5	5	3
LACRT	90070	Q9GZZ8	gi|15187164	LACRITIN	5	30	1
ACTG3	71	P63261	gi|178045		4	12	1
DMBT1	1755	Q9UGM3	gi|169218264	DELETED IN MALIGNANT BRAIN TUMORS 1	4	11	1
FLG	2312	P20930	gi|62122917	FILAGGRIN	4	2	1
HNRNPK	3190	P61978 Q6IBN1 B3KTV0	gi|55958544	HETEROGENEOUS NUCLEAR RIBONUCLEOPROTEIN K	4	11	2
HSPA8*	3312	P11142	gi|5729877	HEAT SHOCK 70kDa PROTEIN 8	4	8	1
KPNB1	3837	Q14974	gi|119615215	KARYOPHERIN (IMPORTIN) BETA 1	4	8	1
LCN1	3933	P31025	gi|4504963	LIPOCALIN 1	4	30	1
LMAN1*	3998	P49257	gi|5031873	LECTIN, MANNOSE-BINDING, 1	4	15	1
PRSS2	5645	P07478 Q5NV56	gi|74353564	PROTEASE, SERINE, 2 (TRYPSIN 2)	4	15	1
ALDH18A1	5832	P54886	gi|76779856	ALDEHYDE DEHYDROGENASE 18 FAMILY, MEMBER A1	4	5	1
NPM3	10360	O75607	gi|5801867	NUCLEOPHOSMIN/NUCLE OPLASMIN, 3	4	12	1
WAC	51322	Q9BTA9	gi|55664165	WW DOMAIN CONTAINING ADAPTOR WITH COILED-COIL	4	5	1
ANKRD24	170961	Q8TF*21	gi|16418357	ANKYRIN REPEAT DOMAIN 24	4	5	1
CALM1	801	Q96HY3 P62158 B4DJ51	gi|61680528	CALMODULIN	3	18	1
COL7A1	1294	Q02388 Q59F16	gi|119585300	COLLAGEN, TYPE VII, ALPHA 1 (EPIDERMOLYSIS BULLOSA, DYSTROPHIC, DOMINANT AND RECESSIVE)	3	1	1
HSPD1	3329	P10809	gi|14326412	HEAT SHOCK 60kDa PROTEIN 1	3	15	2
ME2	4200	P23368 Q9BWL6	gi|5822326	MALIC ENZYME 2, NAD(+)-DEPENDENT	3	5	2
PEX1	5189	O43933	gi|4505725	PEROXISOMAL BIOGENESIS FACTOR 1	3	2	1
PRKAA1	5562	Q13131	gi|29124503	PROTEIN KINASE, AMP-ACTIVATED, ALPHA 1	3	5	1

Gene Symbol	Entrez Gene ID	SwissProt Acc No.	Protein Acc No.	Description	# Pep	% Cov	# Exp
H6PD	9563	O95479	gi | 51859374	CATALYTIC SUBUNIT HEXOSE-6-PHOSPHATE DEHYDROGENASE (GLUCOSE 1-DEHYDROGENASE)	3	3	2
PDIA4	9601	Q549T6 P13667	gi | 37182276	PROTEIN DISULFIDE ISOMERASE FAMILY A, MEMBER 4	3	2	1
COLEC10	10584	Q9Y6Z7	gi | 5453619	COLLECTIN SUB-FAMILY MEMBER 10 (C-TYPE LECTIN)	3	12	1
FOXJ3	22887		gi | 114555879	FORKHEAD BOX J3	3	4	1
ARS2	51593	Q9BXP5	gi | 33150698	ARS2 PROTEIN	3	5	1
FOXJ2	55810	Q9P0K8	gi | 8923842	FORKHEAD BOX J2	3	4	1
UBAP2	55833	Q5T6F2 Q9P0H6	gi | 22325364	UBIQUITIN ASSOCIATED PROTEIN 2	3	3	1
KIAA1529*	57653	Q9P1Z9	gi | 7959325	KIAA1529	3	2	3
LRRC8E	80131	B3KR78	gi | 801893	LEUCINE RICH REPEAT CONTAINING 8 FAMILY, MEMBER E	3	3	1
QRICH2	84074	Q9H0J4	gi | 14149793	GLUTAMINE RICH 2	3	3	1
DPP9*	91039	Q86TI2 Q1ZZB8	gi | 119589606	DIPEPTIDYL-PEPTIDASE 9	3	4	2
LPLUNC1	92747	Q8TDL5	gi | 40807482	NASOPHARGYNEAL RELATED HYPOTHETICAL PROTEIN	3	6	1
DOK7	285489	Q18PE1	gi | 119602869	FLJ33718	3	4	1
SLFN14	342618	P0C7P3	gi | 193788704	ORTHOLOG OF MOUSE SCHLAFEN 10	3	5	1
ENO1	2023	P06733	gi | 4503571	ENOLASE 1	2	6	1
XRCC5	7520	P13010	gi | 119590969	X-RAY REPAIR COMPLEMENTING DEFECTIVE REPAIR IN CHINESE HAMSTER CELLS 5 (DOUBLE-STRAND-BREAK REJOINING; KU AUTOANTIGEN, 80kDa)	2	4	1
WDR1	9948	O75083	gi | 12652891	WD REPEAT DOMAIN 1	2	6	1
NLRP1	22861	Q9C000 Q9H5Z7	gi | 37927559	NLR FAMILY, PYRIN DOMAIN CONTAINING 1	2	1	1
PPA2	27068	Q9H2U2 A6NKL9	gi | 119612395	PYROPHOSPHATASE (INORGANIC) 2	2	1	1
VPS35	55737	Q96QK1	gi | 7022978	VACUOLAR PROTEIN SORTING 35	2	2	1

Proteins Captured with normal αIIb

Gene Symbol	Entrez Gene ID	SwissProt Acc No.	Protein Acc No.	Description	# Pep	% Cov	# Exp
ITGB3*	3690	P05106	gi | 183531	INTEGRIN, BETA 3 (PLATELET GLYCOPROTEIN IIIA, ANTIGEN CD61)	25	42	7

TUBB2C	7284	P49411	gi|20809886	TUBULIN, BETA 2C	17	35	1
DHTKD1	55526	Q96HY7	gi|119606733	DEHYDROGENASE E1 AND TRANSKETOLASE DOMAIN CONTAINING 1	15	36	1
GLUD1	2746	P00367 P14868	gi|183056	GLUTAMATE DEHYDROGENASE 1	15	67	3
DARS	1615	P78371	gi|45439306	ASPARTYL-TRNA SYNTHETASE	14	60	3
LMAN1*	3998	P49257	gi|5031873	LECTIN, MANNOSE-BINDING, 1	12	36	1
PRKAB1	5564	Q9Y478	gi|4506061	PROTEIN KINASE, AMP-ACTIVATED, BETA 1 NON-CATALYTIC SUBUNIT	12	38	1
HSPA5*	3309	P11021 P08246 P43626 P43628	gi|16507237	HEAT SHOCK 70kDa PROTEIN 5 (GLUCOSE-REGULATED PROTEIN, 78kDa)	11	30	1
SCN10A	6336	P43632	gi|110835709	SODIUM CHANNEL, VOLTAGE-GATED, TYPE X, ALPHA	11	5	1
TUBB	10383	P68371	gi|7106439	TUBULIN, BETA 5	11	44	4
TUBB4	23071	Q9BS26	gi|21361322	TUBULIN, BETA 4	10	26	1
ALDH18A1	5832	P54886	gi|76779856	ALDEHYDE DEHYDROGENASE 18 FAMILY, MEMBER A1	9	18	2
DNAJC10*	54431	Q8IXB1 Q01780	gi|24308127	DNAJ (HSP40) HOMOLOG, SUBFAMILY C, MEMBER 10	9	21	4
EXOSC10	5394	P05156	gi|50301239	EXOSOME COMPONENT 10	9	8	1
UGP1	10352	Q9UGM6	gi|48255966	UDP-GLUCOSE PYROPHOSPHORYLASE 1	9	33	1
ADPGK	83440	Q9BRR6	gi|31542509	ADP-DEPENDENT GLUCOKINASE	8	22	1
ALAD	210	P13716	gi|248839	AMINOLEVULINATE, DELTA-, DEHYDRATASE	8	22	1
CCT2	10576	P78371	gi|5453603	CHAPERONIN CONTAINING TCP1, SUBUNIT 2 (BETA)	8	39	1
CCT4	10575	P50991	gi|38455427	CHAPERONIN CONTAINING TCP1, SUBUNIT 4 (DELTA)	8	28	1
FARS2	10667	O95363	gi|62898407	PHENYLALANINE-TRNA SYNTHETASE 2	8	24	1
HSPA1A*	3303	B3KTT5	gi|5123454	HEAT SHOCK 70kDa PROTEIN 1A	8	19	1
HSPA1B	3304	P08107	gi|167466173	HEAT SHOCK 70kDa PROTEIN 1B	8	21	1
HSPA9	3313	P38646	gi|12653415	HEAT SHOCK 70kDa PROTEIN 9B (MORTALIN-2)	8	17	2
NUDT19	390916	A8MXV4	gi|157739940	NUDIX (NUCLEOSIDE DIPHOSPHATE LINKED MOIETY X)-TYPE MOTIF 19	8	36	1

AKR7A2	8574	O43488	gi|41327764	ALDO-KETO REDUCTASE FAMILY 7, MEMBER A2 (AFLATOXIN ALDEHYDE REDUCTASE)	7	37	1
CHD9	80205	Q3L8U1	gi|95147342	CHROMODOMAIN HELICASE DNA BINDING PROTEIN 9	7	2	1
FAM175B	23172		gi|148529023	UNKNOWN PROTEIN LOC23172	7	14	1
KIF14	9928	Q15058	gi|7661878	KINESIN FAMILY MEMBER 14	7	4	1
NT5DC2	22978	A8K6K2	gi|12597653	5'-NUCLEOTIDASE DOMAIN CONTAINING 2	7	36	2
P15RS	55197	Q96P16	gi|142385371	REGULATION OF NUCLEAR pre-mRNA DOMAIN CONTAINING 1A	7	20	1
PDLIM1	9260	Q9Y3C6 Q9NR12	gi|13994151	PDZ AND LIM DOMAIN 1 (ENIGMA)	7	37	1
PM20D2	135293	Q8IYS1	gi|58082085	AMINOACYLASE 1-LIKE 2	7	15	1
POLDIP2	26073	Q9Y2S7 Q9BVV8	gi|7661672	POLYMERASE (DNA-DIRECTED), DELTA INTERACTING PROTEIN 2	7	26	1
TF*	7018	P02787	gi|553788	TRANSFERRIN	7	12	1
ACTN4	604638		gi|2804273	ACTININ, ALPHA 4	6	9	1
ATXN2L*	11273	Q8WWM7	gi|119572372	ATAXIN 2-LIKE	6	9	1
CCT7	10574	Q99832	gi|62896515	CHAPERONIN CONTAINING TCP1, SUBUNIT 7 (ETA)	6	23	1
CNDP2	55748	Q96KP4	gi|8922698	CNDP DIPEPTIDASE 2 (METALLOPEPTIDASE M20 FAMILY)	6	11	1
FLJ12529	79869	Q8N684	gi|24432016	PRE-MRNA CLEAVAGE FACTOR I, 59 kDa SUBUNIT	6	12	1
PBEF1	10135	P43490	gi|55960735	PRE-B-CELL COLONY ENHANCING FACTOR 1	6	4	1
PPP1R9A	55607	Q9ULJ8	gi|261244899	PROTEIN PHOSPHATASE 1, REGULATORY (INHIBITOR) SUBUNIT 9A, 5 isoforms	6	5	1
RB1CC1	9821	Q8TDY2	gi|134304845	RB1-INDUCIBLE COILED-COIL 1	6	3	1
SERBP1	26135	Q8NC51 Q9H707	gi|66346679	SERPINE1 MRNA BINDING PROTEIN 1	6	16	1
TXNDC4	23352	Q8WXW3 Q5T4S7 Q9NP58	gi|119579327	THIOREDOXIN DOMAIN CONTAINING 4 (ENDOPLASMIC RETICULUM)	6	35	3
ACLY	47	P53396	gi|38569423	ATP CITRATE LYASE	5	3	1
ACTB	60	Q1KLZ0	gi|14250401	ACTIN, BETA	5	22	3
CTTN	2017		gi|2498954	CORTACTIN	5	4	1
CUL-5	8065	Q93034	gi|67514034	CULLIN 5	5	5	1
FHL1	2273	Q13642	gi|3851650	FOUR AND A HALF LIM	5	3	1

GPHN	10243	Q9NQX3	gi|10880983	DOMAINS 1 GEPHYRIN ISOFORM 1	5	8	1
HNRPH1	3187	P31943	gi|5031753	HETEROGENEOUS NUCLEAR RIBONUCLEOPROTEIN H1	5	16	1
HSPA8*	3312	P11142	gi|10880983	HEAT SHOCK 70kDa PROTEIN 8	5	8	3
IDH3A	3419	P50213	gi|5031777	ISOCITRATE DEHYDROGENASE 3 (NAD+) ALPHA	5	13	1
PRKAG1	5571	P54619	gi|2230863	PROTEIN KINASE, AMP-ACTIVATED, GAMMA 1 NON-CATALYTIC SUBUNIT	5	27	1
RILPL1	353116	Q5EBL4	gi|30315660	RAB INTERACTING LYSOSOMAL PROTEIN-LIKE 1	5	12	1
SAP130	79595	Q9H0E3	gi:25579126	SIN3A-ASSOCIATED PROTEIN, 130kDa	5	3	1
WARS2	80139	Q9H7S9	gi|7710154	TRYPTOPHANYL TRNA SYNTHETASE 2	5	19	1
ADCY6	112	O43306	gi|168480141	ADENYLATE CYCLASE 6	4	3	1
C5orf25	375484	Q8NDZ2	gi|196259795	FLJ44216 PROTEIN	4	8	1
CARS2	79587	Q9HA77	gi|119618821	HYPOTHETICAL PROTEIN FLJ39378	4	10	1
CIT	11113	O14578	gi|32698687	CITRON (RHO-INTERACTING, SERINE/THREONINE KINASE 21)	4	2	1
EEF2K	29904	O00418	gi|9558749	EUKARYOTIC ELONGATION FACTOR-2 KINASE	4	4	1
FLJ22184	80164	Q9H6K5	gi|239757129	HYPOTHETICAL PROTEIN FLJ22184	4	5	1
FLNA	2316	P21333	gi|57284166	FILAMIN A, ALPHA (ACTIN BINDING PROTEIN 280)	4	2	2
FRMPD1	22844	Q5SYB0	gi|239582740	FERM AND PDZ DOMAIN CONTAINING 1	4	3	1
GOPC	57120	Q9HD26	gi|9966877	GOLGI ASSOCIATED PDZ AND COILED-COIL MOTIF CONTAINING	4	12	1
HMGCS1	3157	Q01581	gi|53734504	3-HYDROXY-3-METHYLGLUTARYL-COENZYME A SYNTHASE 1 (SOLUBLE)	4	14	1
HNRNPL*	3191	P14866	gi|133274	HETEROGENEOUS NUCLEAR RIBONUCLEOPROTEIN L	4	11	2
HTRA2	27429	O43464	gi|21614538	HTRA SERINE PEPTIDASE 2	4	16	1
NAGK	55577	Q9UJ70	gi|6491737	N-ACETYLGLUCOSAMINE KINASE	4	10	1
PKM2*	5315	P14618	gi|31416989	PYRUVATE KINASE,	4	16	1

Gene		UniProt	gi	Protein Name			
				MUSCLE			
		Q05940					
PRDX3	10935	P30048	gi|14250063	PEROXIREDOXIN 3	4	20	1
SF1*	7536	Q15637	gi|46362557	SPLICING FACTOR 1	4	5	1
TIMM50	92609	Q3ZCQ8	gi|48526509	TRANSLOCASE OF INNER MITOCHONDRIAL MEMBRANE 50 HOMOLOG	4	6	1
AER61	285203		gi|39930530	AER61 C3orf64 GLUCOSYLTRANSFERASE	3	6	1
CSNK2A2	1459	Q14012	gi|4503097	CASEIN KINASE 2, ALPHA PRIME POLYPEPTIDE	3	6	1
DPP9*	91039	Q86TI2	gi|114657671	DIPEPTIDYL-PEPTIDASE 9	3	2	1
DVL2	1856	O14641	gi|55665917	DISHEVELLED, DSH HOMOLOG 2 (DROSOPHILA)	3	2	1
ELMO1	9844	O60895	gi|86788139	ENGULFMENT AND CELL MOTILITY 1	3	5	1
GAPDH	2597	P04406 Q16678	gi|31645	GLYCERALDEHYDE-3-PHOSPHATE DEHYDROGENASE	3	18	1
KIAA0895	23366	Q8NCT3	gi|154426319	KIAA0895 PROTEIN	3	6	1
LUC7L2	51631	Q9Y383	gi|4929587	CGI-59 PROTEIN	3	5	1
MPO	4353	P05164	gi|88180	MYELOPEROXIDASE	3	5	2
PEG10	23089	Q86TG7	gi|94421473	PATERNALLY EXPRESSED 10	3	11	1
RPLP0	6175	P05388 Q9NQX7	gi|12654583	RIBOSOMAL PROTEIN, LARGE, P0	3	12	1
SEC13	6396	A8MV37	gi|119584482	SEC13-LIKE 1 (S. CEREVISIAE)	3	11	1
SEC23A	10484	Q15436 Q92736	gi|22477159	SEC23 HOMOLOG A (S. CEREVISIAE)	3	3	1
SHROOM3	57619	Q8TF72	gi|57284166	SHROOM3 F-ACTIN BINDING PROTEIN	3	2	4
UBR4	23352		gi|9367763	ZINC FINGER, UBR1 TYPE 1	3	3	1
A2M	2	P01023	gi|177872	ALPHA-2-MACROGLOBULIN	2	1	1
ABCA13	154664	Q86UQ4	gi|8928549	ATP-BINDING CASSETTE, SUB-FAMILY A (ABC1), MEMBER 13	2	5	2
CORO1A	11151	P31146	gi|5902134	CORONIN, ACTIN BINDING PROTEIN, 1A	2	4	1
KIAA1529*	57653	Q9P1Z9	gi|7959325	KIAA1529	2	2	4
MAP3K7IP2	23118	Q9NYJ8	gi|14149669	MITOGEN-ACTIVATED PROTEIN KINASE KINASE KINASE 7 INTERACTING PROTEIN 2	2	2	1
RANBP10	57610	Q6VN20	gi|40538736	RAN BINDING PROTEIN 10	2	4	1
RAVER1*	125950	Q8IY67	gi|123173757	RAVER1	2	4	1
TUBA1A	203068	P07437	gi|340021	TUBULIN, ALPHA	2	2	3
ZNF703	80139		gi|13376610	ZINC FINGER PROTEIN 703	2	3	1

Table 1. Proteins captured with αIIb in megakaryocytes and HEK293 cells. Results are separated according to the αIIb subunit they were captured with. Column labels: Gene

Symbol, EntrezGene ID, Protein Accession Number and Description are from the NCBI database. SwissProt Accession Number is from the UniProt database. Number of Unique Peptides is cumulative from all experiments. Coverage percent is cumulative for all experiments. Tally is shown of the total number of experiments in which a protein was identified (No Expts), and whether captured by histidine tag/Ni affinity (Ni-His) or by crosslinking (X-link). Presence or absence in a recently published expression study (HaemAtlas) is indicated. * Proteins captured by both normal and mutant αIIb subunits.

3.2 Gene Ontology analysis

Gene Ontology (GO) analysis using the DAVID Bioinformatics Resources(Dennis, Sherman et al. 2003; Huang, Sherman et al. 2008) revealed enrichment for protein functions related to processing and trafficking, and ER, Golgi or vesicle components (Figure 3). Comparison of the proteins isolated with the normal αIIb subunits *vs* with the αIIbR858G/R859G subunits showed similar distributions of their localization and molecular functions (**Table 2**). Notably, the αIIbR858G/R859G subunits captured a greater percentage of these types of proteins, suggesting that a greater percentage of the αIIbR858G/R859G subunits were associated with the ER, Golgi and vesicles. Comparison of our data set to a recently published analysis of gene expression in megakaryocytes(Watkins, Gusnanto et al. 2009) showed that approximately 70% of the proteins identified herein as potentially interacting with αIIb were identified as expressed in the megakaryocyte transcriptome.

GO function/location	% of total proteins	
	αIIb	αIIbR858G/R859G
Protien transport	31	49
Stress Caperone	21	34
Vesicle part	6	14
ER or Golgi part	19	21
Organelle part	27	41
Cytoskeleton	21	29
ATP/GTP binding	31	45

Table 2. Distribution of captured proteins into Gene Ontology categories. Some proteins appear in more than one category.

Despite the similarity in distributions into GO categories pertaining to protein processing and localization, there were only 14 proteins in common between the normal αIIb and αIIbR858G/R859G captured proteins (**Table 1**). This may indicate a difference in the relative amount of time spent by the normal and mutant subunits in the protein processing environment. One protein, DNAJC10, was captured in all experiments by both αIIb and αIIbR858G/R859G. Like other DNAJ proteins, DNAJC10 contains a binding domain for the chaperone BiP, but is unique in that its second domain has four protein-disulfide-isomerase (PDI) consensus sequences. (Cunnea, Miranda-Vizuete et al. 2003; Dong, Bridges et al. 2008) Because disulfide bond rearrangement is important for both biogenesis and function of αIIbβ3, we investigated the putative interaction between αIIb and DNAJC10. To our knowledge, DNAJC10 has not previously been reported to interact with αIIb or β3.

3.3 DNAJC10 interacts with αIIbβ3 during biogenesis

DNAJC10 coimmunoprecipitated with αIIb and β3 from UCB derived megakaryocytes using anti-αIIb mAbs 10E5, B1B5, M148 and CA3, and the anti β3 mAb 7H2. DNAJC10 either interacted with αIIb and β3 directly or was part of a complex with them (**Figure 3**). Because DNAJC10 was captured by the αIIbR858G/R859G subunit, we explored the possibility that DNAJC10 interacted with αIIb prior to αIIbβ3 complex formation and αIIb cleavage to its mature form. We have previously shown that pro-αIIb is degraded by the proteasome and that proteasome inhibition leads to an increase of pro-αIIb within the cells. (Mitchell, Li et al. 2006) The undegraded pro-αIIb is trapped in a "pre-degradation" state in which normally transient protein interactions, which usually lead to degradation, may become more long-lived and may be captured by co-immunoprecipitation. Incubation of megakaryocytes with MG132 resulted in increased DNAJC10 co-immunoprecipitation with αIIb by all mAbs, but particularly M148 and CA3. Thus, DNAJC10 may associate with αIIb early in biogenesis, before excess pro-αIIb is targeted to the proteasome.
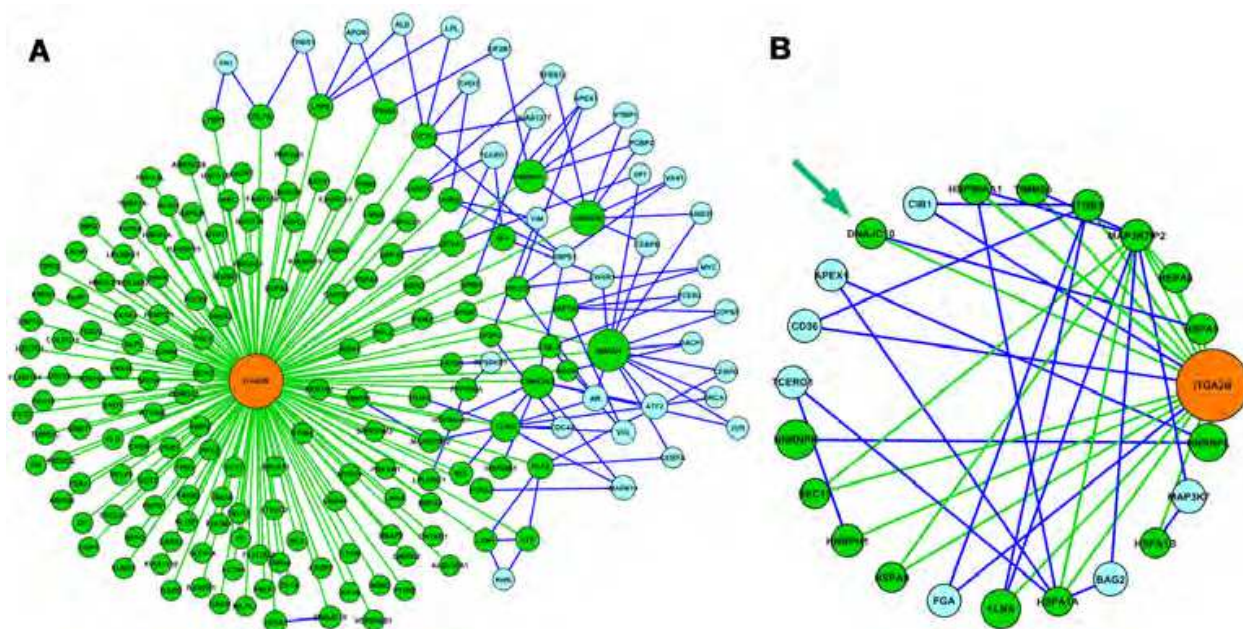
Fig. 3. Network derived from Table 1 data. Proteins are represented as nodes (circles) labeled with their gene symbol, and putative protein interactions with αIIb are indicated by thin green connecting lines. Thick blue lines and blues circles represent interactions or proteins, respectively, retrieved from online databases (Intact and NCBI) using the Cytoscape software. Arrow indicates DNAJC10. Figure prepared using Cytoscape.

To test this possibility we used a panel of conformation-specific mAbs that we have previously used to track the conformational changes of αIIb as it proceeds through biogenesis (**Figure 3**).(Mitchell, Li et al. 2007) Specifically: mAb10E5 binds to the αIIb head region and recognizes both the pro-αIIbβ3 and mature αIIbβ3 complex; mAb 7E3 binds to the β3 head region and also recognizes both the pro- and mature complex; mAb B1B5 binds to the αIIb tail and preferentially recognizes pro-αIIb and pro-αIIbβ3 complex, and mAb M148 preferentially recognizes mature αIIbβ3 but its epitope is not known.(Mitchell, Li et al.

2007) To determine whether DNAJC10 interacts with αIIb during a specific stage of biogenesis, αIIb was immunoprecipitated from megakaryocytes in the presence of MG132 using this panel of conformation-specific mAbs. DNAJC10 was most strongly coimmunoprecipitated by mAb B1B5, suggesting that DNAJC10 preferentially interacts with pro-αIIb or the pro-αIIbβ3 complex. In contrast, DNAJC10 coimmunoprecipitated less well with mAb M148, suggesting less interaction with mature αIIb. DNAJC10 also interacted with the precursor and/or mature αIIbβ3 complex, since it coimmunoprecipitated with the complex-specific mAb10E5. Since the ratio of pro-αIIbβ3 to mature αIIbβ3 is small in megakaryocytes,(Mitchell, Li et al. 2007) this binding pattern is consistent with DNAJC10 having bound preferentially to the small amount of pro-αIIbβ3 present in the cells. Together these findings suggest that DNAJC10 preferentially interacted with pro-αIIb and the pro-αIIbβ3 complex, rather than the mature complex.
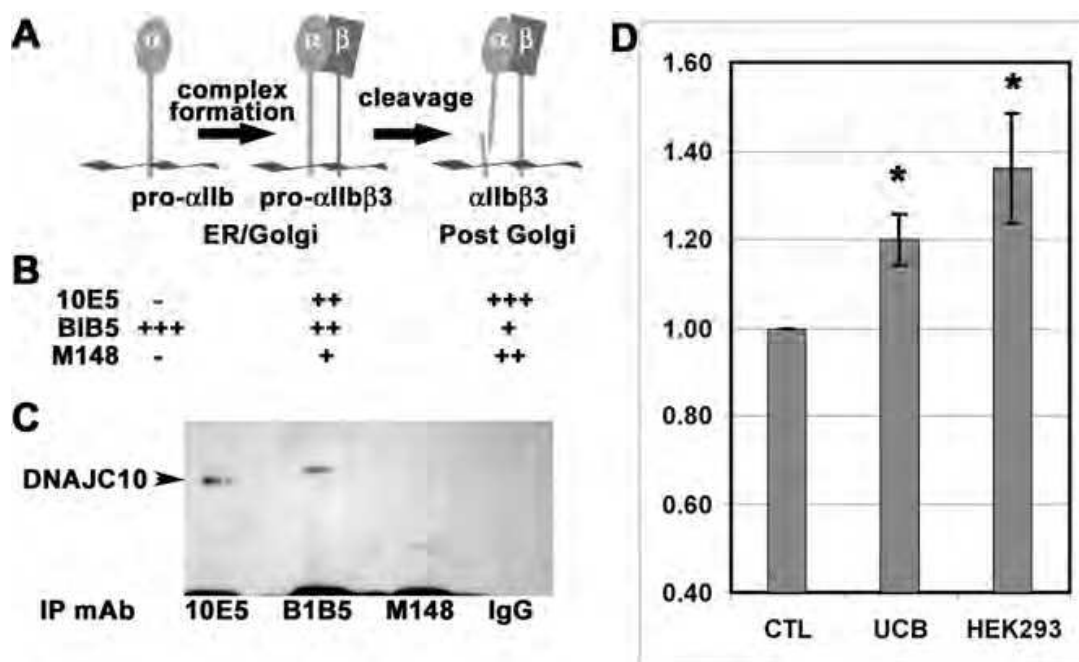
Fig. 4. Interaction of DNAJC10 with αIIbβ3 during biogenesis. A) Schematic of changing conformations of αIIbβ3 as it progresses through biogenesis. B) Changing specificity of 3 mAbs against αIIb as it progresses through distinct conformations during biogenesis. B1B5 preferentially recognizes pro-αIIb, while M148 shows preference for mature αIIb, and 10E5 recognizes the heterodimer complex.C) Immunoprecipitation and Western blot of proteins isolated from megakaryocytes, as described in text. DNAJC10 coimmunoprecipitated preferentially with αIIb that was pulled down by 10E5 and B1B5, but not M148, suggesting that DNAJC10 preferentially interacts with pro-αIIb and pro-αIIbβ3. The last lane is an IgG control. **D)** siRNA mediated knockdown of DNAJC10 increased surface expression of αIIbβ3 as measured by flow cytometry using an Alexa647-labeled anti-αIIbβ3 mAb (10E5). Expression was increased by 25 +\- 11% (p=0.02, n=4) in UCB-derived megakaryocytes (UCB) and by 35 +\- 12% (p=0.01, n=3) in HEK293 cells (HEK293) compared to control siRNA transfection (CTL).

3.4 DNAJC10 depletion increases surface expression of αIIbβ3

To determine whether the αIIb-DNAJC10 interaction had physiological relevance, we assessed its impact on the surface expression of αIIbβ3 in megakaryocytes. siRNA mediated knockdown of DNAJC10 was performed on both human megakaryocytes derived from UCB and on HEK293 cells expressing normal αIIb and β3. At least an 80% decrease in RNA level was achieved (data not shown). Knockdown of DNAJC10 increased αIIbβ3 surface expression on megakaryocytes by 25% +/- 11% (n = 4, p = 0.02), and on HEK293 cells expressing αIIbβ3 by 35% +/- 12% (n=4, p = 0.01) (**Figure 3D**).

3.5 Intracellular localization of DNAJC10 in megakaryocytes

DNAJC10 was localized within megakaryocytes by immunofluorescence microscopy (Figure 5). The distribution of DNAJC10 was compared to that of αIIb, β3, and the ER and Golgi compartments. Both αIIb and β3 were distributed throughout the ER as well as on the cell surface. DNAJC10 had a diffuse punctate distribution in the periphery of the cell, away from the nucleus, and colocalized with only a portion of aIIb and β3, consistent with their presumably transient interaction. There was partial overlap between the ER marker calnexin and DNAJC10, suggesting that part of the DNAJC10 distribution is outside the ER or at least
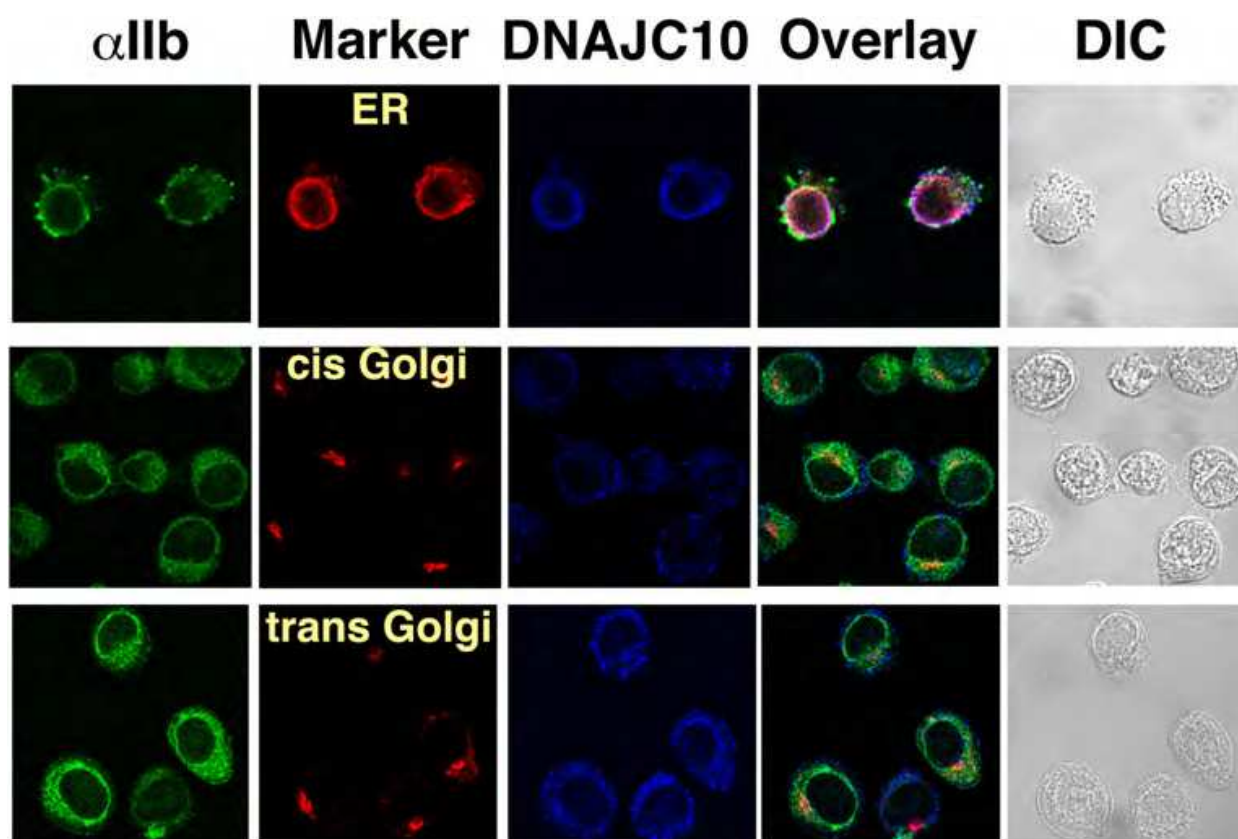
Fig. 4. Intracellular localization of DNAJC10. Cultured megakaryocytes were fixed and immunostained as described in the text. DNAJC10 (Blue) exhibited a punctate staining in the periphery of the cells, away from the nucleus. There was partial overlap of DNAJC10 with calnexin (Red) staining. αIIb (Green) was distributed throughout the ER and cell surface. While αIIb partially colocalized with the cis- and trans-Golgi, DNAJC10 did not.

separate from the distribution of calnexin in the ER. This finding was surprising since DNAJC10 has the ER-retention signal KDEL. DNAJC10 did not localize with markers for the cis- or trans-Golgi compartments.

4. Discussion

We have used a proteomics approach to identify novel proteins interacting with αIIb in megakaryocytes. Two different constructs of αIIb, representing normal αIIb and pro-αIIb subunits, were used to capture proteins interacting with both nascent and mature subunits. Megakaryocytes were derived from human UCB and used on day 8, which in our system yields high expression αIIbβ3 on the surface but no proplatelet formation.(Mitchell, Li et al. 2006) In all, 163 proteins were identified as potentially interacting with αIIb subunits; 98 were captured with normal αIIb and 79 with aIIbR858/G859G, with 14 overlapping (Table 1). Day 8 megakaryocytes express very high amounts of αIIb, most of which is mature αIIbβ3, resulting in a relatively small proportion of nascent αIIb. However, a large proportion of the mutant aIIbR858/G859G subunits are retained within the cell and degraded. Thus the difference between the two protein lists could partly be due to their differences in localization within the cell. This may be reflected in the larger proportion of ER and Golgi related proteins that were captured with the mutant subunit (**Table 2**). Only a few intracellular proteins have been reported to interact with αIIb and αIIbβ3, most notably talin, calnexin, and calreticulin (Intact and NCBI). Our two-step protein capture method was designed to isolate proteins with low affinity binding to αIIb, such as calnexin, while screening out higher affinity binding proteins, such as talin and β3. In accord with this expectation, both talin and β3 were identified in both the control and experimental lanes, and so were excluded from the final interaction list, while calnexin and calreticulin were identified only in the experimental lanes. Surprisingly, while DNAJC10 readily coimmunoprecipitates with αIIbβ3 from megakaryocytes, we have been unable to replicate this finding in HEK293 cells transfected with αIIb and β3, despite an abundance of DNAJC10 in HEK293 cells (data not shown). While this is in no way conclusive, it is suggestive of cell-specific interaction of αIIbβ3 and DNAJC10 in megakaryocytes. Comparison of our experimental results with previously reported platelet proteomic data and αIIbβ3 interaction data showed good correlation. About 70% of the proteins identified in our screens were reported as "present" in platelets in the Haem Atlas, a proteomic analysis of platelet protein content(Watkins, Gusnanto et al. 2009).

Two protein capturing strategies were used, each with strengths and weaknesses. The two-cell pull-down assay using Ni beads to capture poly-histidine-tagged αIIb, allowed the use of mutant cDNA constructs, such as αIIbR858G/R859G, as bait. However, by introducing a protein synthesized in HEK293 cells as bait, there was the potential for false positive identification of proteins that associated with αIIb in the HEK293 cells but not in megakaryocytes. Since the interactions of chaperone proteins are typically of low affinity, these proteins were most likely cleared by the washing steps and did not appear in the control lanes. Another source of false positives was non-specific binding to the Ni beads. Proteins with poly-His sequences (such as DEAH boxes) or naturally occurring Ni binding activity (such as keratin) could have bound to the beads, constituting false positives. However, virtually all of these potential false positives appeared in the control lanes as well and were excluded from analysis. The photoreactive crosslinking assay was intended to

capture proteins in situ with αIIb in megakaryocytes. While crosslinking experiments typically produce high numbers of false positives, in our experiments we identified low numbers of proteins from both the experimental and control lanes. The low yield may be due in part to the short crosslinking time used. We found that more than 15 minutes of UV exposure caused excessive protein degradation, while shorter exposure resulted in low crosslinking activity.

Of the proteins captured using both αIIb and αIIbR858G/R859G the Hsp40-type chaperone protein, DNAJC10 (ERdj5), was notable due to its disulfide isomerase activity, since both αIIb and β3 require disulfide bond rearrangement for both biogenesis and function. (Shen, Meunier et al. 2002; Cunnea, Miranda-Vizuete et al. 2003; Dong, Bridges et al. 2008) Among its several functions, the ER chaperone protein BiP protects nearly-folded proteins against aggregation by binding to exposed hydrophobic patches.(Hendershot 2004) The Hsp40 chaperones bind to BiP and increase its efficiency of ATP hydrolysis, which allows BiP to release its substrate. DNAJC10 has been shown to be induced during ER stress, and may assist in delivering misfolded ER proteins to the proteasome for degradation.(Shen, Meunier et al. 2002; Cunnea, Miranda-Vizuete et al. 2003; Dong, Bridges et al. 2008)

DNAJC10 coimmunoprecipitated with both αIIb and β3 subunits in megakaryocytes, suggesting that it may bind the αIIbβ3 complex. The immunoprecipitation pattern obtained using a panel of conformation-specific mAbs(Mitchell, Li et al. 2007) indicated that DNAJC10 preferentially interacted with pro-αIIb or pro-αIIbβ3 rather than mature αIIbβ3. Together these findings suggest that DNAJC10 interacted with pro-αIIb up to the point of complex formation, but not after pro-αIIb cleavage (Figure 2). Thus DNAJC10 appears to be present and interacting with αIIb at a critical decision point during αIIbβ3 biogenesis, i.e. when pro-αIIb will either form the mature αIIbβ3 complex or be targeted to degradation.

Surprisingly, the distribution of DNAJC10, which has a KDEL ER-localization signal, was not confined to the ER, as judged by the distribution of calnexin. To determine if DNAJC10 was cycling to the Golgi and back, as many ER packaging proteins do, we looked for colocalization of DNAJC10 with cis and trans Golgi markers, and found none. The identity of the organelle(s) where DNAJC10 resides remains to be determined.

Depletion of DNAJC10 by siRNA resulted in an increase in surface expression of αIIbβ3 on both human megakaryocytes and transfected HEK293 cells (**Figure 2D**) Since DNAJC10 depletion led to an increase in αIIbβ3 surface expression, it appears to be a negative regulator of αIIbβ3 surface expression. These findings make DNAJC10 an interesting and potentially targetable protein for perturbing αIIbβ3 biogenesis.

5. Conclusion

While the details of DNAJC10-αIIb interaction remain to be investigated, the current findings provide proof of principle that manipulation of early events in αIIb biogenesis can result in altered expression levels of the mature αIIbβ3 receptor, thereby setting a precedent for a novel approach to integrin-related therapy. These studies also support the validity of the data set, although other putative interactions must be explored for greater validation. We hope that the data set created will be a useful tool for studying integrin and megakaryocyte biology.

By deciphering the αIIbβ3 biogenesis pathway we hope to gain an inroad into controlling the level of αIIbβ3 expression on platelets with the long-term goal of developing novel anti-thrombotic therapies. These types of therapy would not just inactivate the circulating platelets, but would modulate the megakaryocytes to make less adhesive platelets. One can imagine a scenario where patients at high risk of heart attack or stroke could be maintained on a drug that decreases their platelet αIIbβ3 expression. Below a certain level of expression, platelet activation and aggregation would be diminished but not completely eliminated, resulting in an overall decrease in platelet thrombus formation but not complete loss of platelet function. This type of therapy could potentially have a greater safety profile than current therapies that summarily inactivate circulating platelets.

This study also assembles some of the wide range of research methods available to hematology research. No single technique could have discovered, validated and explored the function of DNAJC10 in megakaryocytes: rather, a broad range of methods was required. This wide variety is part of what makes research exciting and underscores the benefits of collaboration.

6. Acknowledgement

7. References

Bray, P. F., J. P. Rosa, et al. (1986). "Biogenesis of the platelet receptor for fibrinogen: Evidence for separate precursors for glycoproteins IIb and IIIa." Proc Natl Acad Sci USA 83: 1480-1484.

Cline, M. S., M. Smoot, et al. (2007). "Integration of biological networks and gene expression data using Cytoscape." Nat. Protocols 2(10): 2366-2382.

Cunnea, P. M., A. Miranda-Vizuete, et al. (2003). "ERdj5, an Endoplasmic Reticulum (ER)-resident Protein Containing DnaJ and Thioredoxin Domains, Is Expressed in Secretory Cells or following ER Stress." Journal of Biological Chemistry 278(2): 1059-1066.

De Luca, G., G. Ucci, et al. (2009). "Benefits from small molecule administration as compared with abciximab among patients with ST-segment elevation myocardial infarction treated with primary angioplasty: a meta-analysis." J Am Coll Cardiol 53(18): 1668-73.

Dennis, G., B. Sherman, et al. (2003). DAVID: Database for Annotation, Visualization, and Integrated Discovery. Genome Biol 4(5):P3.

Dong, M., J. P. Bridges, et al. (2008). "ERdj4 and ERdj5 Are Required for Endoplasmic Reticulum-associated Protein Degradation of Misfolded Surfactant Protein C." Molecular Biology of the Cell 19(6): 2620-2630.

El.Golli, N., O. Issertial, et al. (2005). "Evidence for a Granule Targeting Sequence within Platelet Factor 4." Journal of Biological Chemistry 280(34): 30329-30335.

Hendershot, L. M. (2004). "The ER function BiP is a master regulator of ER function." Mt Sinai J Med 71(5): 289-97.

Huang, D. W., B. T. Sherman, et al. (2008). "Systematic and integrative analysis of large gene lists using DAVID bioinformatics resources." Nat. Protocols 4(1): 44-57.

King, S. M. and G. L. Reed (2002). "Development of platelet secretory granules." Seminars in Cell & Developmental Biology 13(4): 293-302.

Kolodziej, M. A., G. Vilaire, et al. (1991). "Study of the endoproteolytic cleavage of platelet glycoprotein IIb using oligonucleotide-mediated mutagenesis." J Biol Chem 266: 23499-23504.

Kumarathasan, P., S. Mohottalage, et al. (2005). "An optimized protein in-gel digest method for reliable proteome characterization by MALDI-TOF-MS analysis." Anal Biochem 346(1): 85-9.

Lo, B., L. Li, et al. (2005). "Requirement of VPS33B, a member of the Sec1/Munc18 protein family, in megakaryocyte and platelet {alpha}-granule biogenesis." Blood 106(13): 4159-4166.

Mitchell, W. B., J. Li, et al. (2006). "alphaIIbbeta3 biogenesis is controlled by engagement of alphaIIb in the calnexin cycle via the N15-linked glycan." Blood 107(7): 2713-2719.

Mitchell, W. B., J. Li, et al. (2007). "Mapping early conformational changes in alphaIIb and beta3 during biogenesis reveals a potential mechanism for alphaIIbbeta3 adopting its bent conformation." Blood 109(9): 3725-32.

Quinn, M. J., E. F. Plow, et al. (2002). "Platelet glycoprotein IIb/IIIa inhibitors: recognition of a two-edged sword?" Circulation 106(3): 379-85.

Rosa, J.-P. and R. P. McEver (1989). "Processing and assembly of the integrin, glycoprotein IIb-IIIa, in HEL cells." J Biol Chem 264: 12596-12603.

Shen, Y., L. Meunier, et al. (2002). "Identification and characterization of a novel endoplasmic reticulum (ER) DnaJ homologue, which stimulates ATPase activity of BiP in vitro and is induced by ER stress." J Biol Chem 277(18): 15947-56.

Tiwari, S., J. E. Italiano, Jr., et al. (2003). "A role for Rab27b in NF-E2-dependent pathways of platelet formation." Blood 102(12): 3970-9.

Topol, E. J., A. M. Lincoff, et al. (2002). "Multi-year follow-up of abciximab therapy in three randomized, placebo-controlled trials of percutaneous coronary revascularization." Am J Med 113(1): 1-6.

Watkins, N. A., A. Gusnanto, et al. (2009). "A HaemAtlas: characterizing gene expression in differentiated human blood cells." Blood 113(19): e1-9.
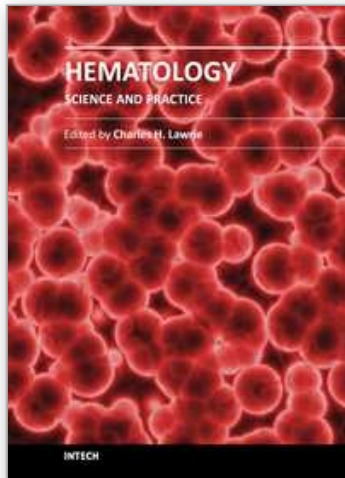
Hematology - Science and Practice

Edited by Dr. Charles Lawrie

Hematology encompasses the physiology and pathology of blood and of the blood-forming organs. In common with other areas of medicine, the pace of change in hematology has been breathtaking over recent years. There are now many treatment options available to the modern hematologist and, happily, a greatly improved outlook for the vast majority of patients with blood disorders and malignancies. Improvements in the clinic reflect, and in many respects are driven by, advances in our scientific understanding of hematological processes under both normal and disease conditions. Hematology - Science and Practice consists of a selection of essays which aim to inform both specialist and non-specialist readers about some of the latest advances in hematology, in both laboratory and clinic.

How to reference

In order to correctly reference this scholarly work, feel free to copy and paste the following:

Amanda Chen, Haiqiang Yu, Haiteng Deng and W. Beau Mitchell (2012). Mechanisms of αIIbβ3 Biogenesis in the Megakaryocyte: A Proteomics Approach, Hematology - Science and Practice, Dr. Charles Lawrie (Ed.), ISBN: 978-953-51-0174-1, InTech, Available from: http://www.intechopen.com/books/hematology-science-and-practice/mechanisms-of-iib-3-biogenesis-in-the-megakaryocyte-a-proteomics-approach

INTECH

open science | open minds